

Emergent short-range repulsion for attractively coupled active particles

Ritwick Sarkar, Urna Basu

S. N. Bose National Centre for Basic Sciences, Kolkata 700106, India

We show that heterogeneity in self-propulsion speed leads to the emergence of effective short-range repulsion among active particles coupled via strong attractive potentials. Taking the example of two harmonically coupled active Brownian particles, we analytically compute the stationary distribution of the distance between them in the strong coupling regime, i.e., where the coupling strength is much larger than the rotational diffusivity of the particles. The effective repulsion in this regime is manifest in the emergence of a minimum distance between the particles, proportional to the difference in their self-propulsion speeds. Physically, this distance of the closest approach is associated to the orientations of the particles being parallel to each other. We show that the physical scenario remains qualitatively similar for any long-range coupling potential, which is attractive everywhere. Moreover, we show that, for a collection of N particles interacting via pairwise attractive potentials, a short-range repulsion emerges for each pair of particles with different self-propulsion speeds. Finally, we show that our results are robust and hold irrespective of the specific active dynamics of the particles.

I. INTRODUCTION

Active self-propelled particles perform persistent motion by consuming energy at an individual level from their environment [1–7]. Examples of such active motion are abundant in nature ranging from bacterial motility [8] to movement of birds or fish [9–13]. Artificially designed active agents like Janus particles also exhibit similar motion [14, 15]. The inherently nonequilibrium nature of active particle motion makes their collective properties far richer than their equilibrium counterparts. Perhaps the most surprising is the propensity of these particles to form clusters in the absence of any attractive force, leading to a range of unusual phenomena including motility-induced phase separation [16–19], collective motion [20–22], and formation of ordered structure [23–25].

Theoretical efforts to uncover the origin of the unusual emergent behaviour in active matter often relies on investigating simple model systems comprising few particles. A first step is to explore the effective interaction between two active particles coupled via some simple potential. The stationary fluctuation of the separation r between a pair of passive particles coupled by a sufficiently attractive potential $V(r)$ is governed by the equilibrium distribution $P(r) \sim e^{-\beta V(r)}$. For active particles, however, no such general form exists, and the effective interaction potential, in general, differs from the underlying interaction [26].

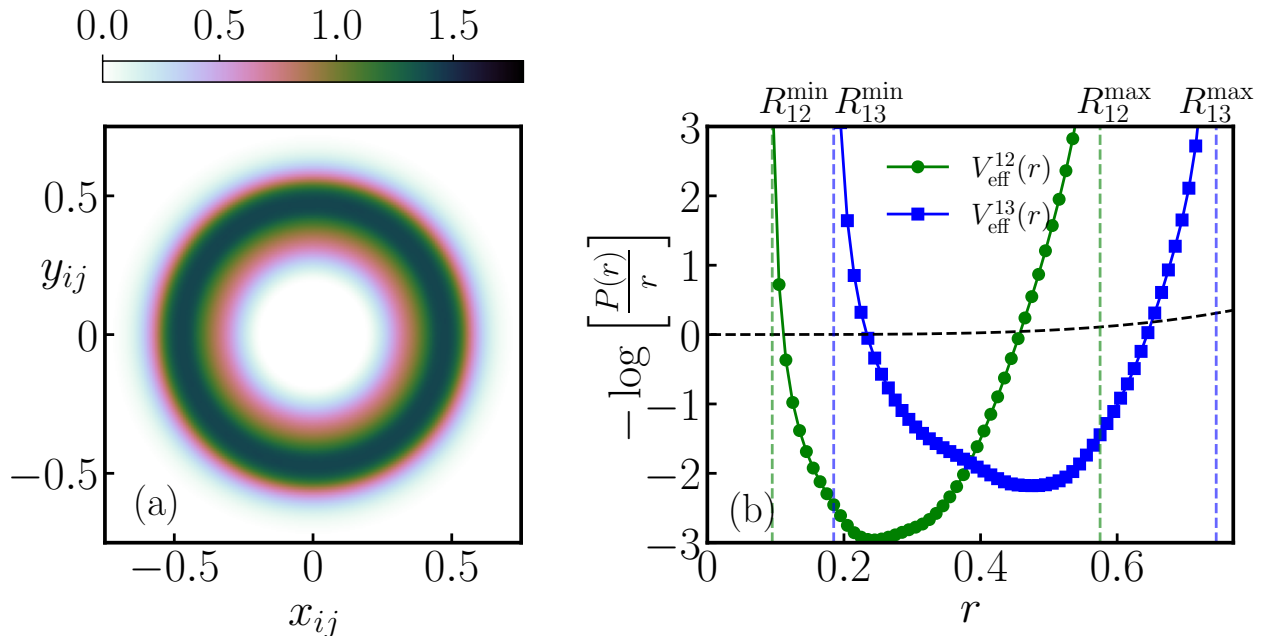


FIG. 1. Multi-particle system ($N = 6$) interacting via a pair-wise quartic potential [see Eq. (19)]: (a) Plot of joint probability distribution $P(x_{13}, y_{13})$ obtained from numerical simulations. (b) Effective pair-wise potential $V_{\text{eff}}^{ij}(r)$ extracted from $P(r_{ij})$. Here we have used $v_i = 3i - 2$, $\kappa = 4$ and $D = 0.02$.

It has recently been shown that an effective attractive interaction emerges between two active particles even in the presence of hardcore repulsion [27–30]. A similar attractive interaction emerges also for two particles coupled via long-range attractive potentials [31]. In fact, the presence of persistence may tune an underlying repulsive recoil interaction into an effective attractive one [32, 33]. Recent studies of pairwise gap statistics in many particle systems indicate that similar attractive interactions also emerge for many particle systems [34]. Such emergent attractive interactions are thought to be the driving element behind most of the unusual collective behaviour of active particles.

In this work, we show that the effective interaction between active particles need not always be attractive. In fact, we propose a generic mechanism to generate an effective pairwise repulsive interaction among active particles that are coupled attractively. It turns out that, the crucial element to generate such a repulsion is the presence of diversity in the self-propulsion speed. Using a simple model, we also analytically characterize this repulsive interaction, which, to the best of our knowledge, has not been observed before.

II. MODEL AND RESULT

We consider a collection of N overdamped active Brownian particles (ABP) [35–37] moving in two-dimensions. In the absence of any interaction or external force, each particle self-propels along its internal

orientation, which itself evolves stochastically. The set-up comprises particles interacting pairwise via some attractive potential $V(r)$, which depends only on the radial distance r between the two particles. The potential is assumed to be long-ranged and attractive everywhere such that the corresponding force $\mathbf{f}(r) = -\nabla V(r)$ diverges for $r \rightarrow \infty$. The Langevin equations governing the time-evolution of the position $\dot{\mathbf{r}}_i = (x_i, y_i)$ of the i -th particle is given by,

$$\dot{\mathbf{r}}_i = -\sum_{j \neq i}^N \nabla_i V(|\mathbf{r}_i - \mathbf{r}_j|) + v_i \hat{\mathbf{n}}_i, \quad (1)$$

where, v_i denotes the self-propulsion speed of the i -th particle, and $\hat{\mathbf{n}}_i = (\cos \theta_i, \sin \theta_i)$ indicates its internal orientation. The orientation of each particle evolves via a rotational Brownian motion, $\dot{\theta}_i(t) = \sqrt{2D_i} \eta_i(t)$, where $\{\eta_i(t)\}$ denote independent white noises with correlation $\langle \eta_i(t) \eta_j(t') \rangle = \delta_{ij} \delta(t - t')$ and D_i denotes the rotational diffusion coefficient of the i -th particle.

We find that, surprisingly, in the strong coupling regime, i.e., when coupling strength is significantly higher than the rotational diffusivity of the particles, an effective short-range repulsion emerges between each pair of particles when their self-propulsion speeds are not equal. This short-range repulsion is manifest in the emergence of a minimum distance between each pair of particles. This is illustrated in Fig. 1(a) for a set of particles with pairwise quartic coupling. An exact expression for the distribution of the pairwise distance $r_{ij} = |\mathbf{r}_i - \mathbf{r}_j|$ is derived for the scenario where the particles are coupled to each other harmonically, i.e., $V(r) = kr^2/2$. We show that, in this case, the distance r_{ij} remains bounded in the region,

$$R_{ij}^{\min} \equiv \frac{|v_i - v_j|}{Nk} \leq r_{ij} \leq R_{ij}^{\max} \equiv \frac{(v_i + v_j)}{Nk}, \quad (2)$$

with the distribution satisfying the scaling form,

$$P(r_{ij}) = \frac{1}{R_{ij}^{\max}} \mathcal{R}_{ij} \left(\frac{r_{ij}}{R_{ij}^{\max}} \right). \quad (3)$$

The scaling function is different for each pair of particles,

$$\mathcal{R}_{ij}(u) = \frac{2u}{\pi \sqrt{(1-u^2)(u^2 - \ell_{ij}^2)}}, \quad (4)$$

which depends on the ratio $\ell_{ij} = R_{ij}^{\min}/R_{ij}^{\max}$.

The corresponding marginal distribution for the x -component of the distance is also computed exactly, and can be expressed in a scaling form,

$$P(x_{ij}) = \frac{1}{R_{ij}^{\max}} \mathcal{F}_{ij} \left(\frac{x_{ij}}{R_{ij}^{\max}} \right), \quad (5)$$

with the scaling function,

$$\mathcal{F}_{ij}(u) = \begin{cases} \frac{2i}{\pi^2 \sqrt{\ell_{ij}^2 - u^2}} \left[K\left(\frac{1-u^2}{\ell_{ij}^2 - u^2}\right) \right. \\ \left. - \sqrt{\frac{\ell_{ij}^2 - u^2}{1-u^2}} K\left(\frac{\ell_{ij}^2 - u^2}{1-u^2}\right) \right] & \text{for } |u| < \ell_{ij}, \\ \frac{2}{\pi^2 \sqrt{u^2 - \ell_{ij}^2}} K\left[\frac{1-u^2}{\ell_{ij}^2 - u^2}\right] & \text{for } \ell_{ij} < |u| < 1, \end{cases} \quad (6)$$

where $K(u)$ denotes the complete Elliptic integral of the first kind [38]. This marginal distribution is bimodal in shape, with a minimum at $x_{ij} = 0$ and two peaks at $x_{ij} = \pm R_{ij}^{\min}$, which is a signature of the emergent repulsion [see Fig 2]. Equations (3)- (6) are one of the central results of this work.

This phenomenon can also be generalized for non-linear coupling. In fact, it turns out that, the distance between two strongly active particles coupled by a generic potential $V(r)$, which is attractive everywhere, must be bounded within the region R^{\min} and R^{\max} that satisfies the following relation,

$$f(R^{\min}) = \frac{|v_1 - v_2|}{2} \quad \text{and} \quad f(R^{\max}) = \frac{v_1 + v_2}{2}. \quad (7)$$

Here $f(r)$ denotes the norm of the force acting between the pair of active particles. Similar behaviour is observed for $N > 2$ particles coupled with anharmonic potential, although analytical results are hard to obtain. Figure 1(b) shows a plot of the effective potential extracted from numerical simulations.

The remarkable feature of an emergent short-range repulsion, for particles which are coupled by long-range attractive potentials, is a phenomenon unique to the active particles, and is not achievable by their passive counterparts. Moreover, these results remain qualitatively same irrespective of the specific nature of the underlying active dynamics. In the following we provide the main computational steps leading to the above results. We start with the case of $N = 2$ harmonically coupled active Brownian particles.

A. Binary system ($N = 2$)

To understand the behaviour of the two-particle system, it is convenient to rewrite Eq. (1) in terms of the relative distance $\mathbf{r} = \mathbf{r}_1 - \mathbf{r}_2$ and center of mass $\mathbf{q} = \frac{1}{2}(\mathbf{r}_1 + \mathbf{r}_2)$,

$$\dot{\mathbf{r}} = -2k\mathbf{r} + v_1\hat{\mathbf{n}}_1 - v_2\hat{\mathbf{n}}_2, \quad \text{and} \quad \dot{\mathbf{q}} = v_1\hat{\mathbf{n}}_1 + v_2\hat{\mathbf{n}}_2. \quad (8)$$

Clearly, the distance $\mathbf{r}(t)$ evolves via a Langevin equation Eq. (8) which describes the motion of a particle in a harmonic potential of stiffness $2k$, subject to a combination of stochastic noises. The presence of

the harmonic trap and bounded nature of the noise ensure that the distance between the particles would eventually reach a stationary state. On the other hand, the center of mass undergoes an unbounded motion. In this work, we focus on the behaviour of the stationary state distribution of the distance between the two particles, in the strongly active regime.

The formal solution of Eq. (8) reads,

$$\mathbf{r}(t) = \int_0^t ds e^{-2k(t-s)} [v_1 \hat{n}_1(s) - v_2 \hat{n}_2(s)]. \quad (9)$$

The orientation vectors $\hat{n}_i = (\cos \theta_i, \sin \theta_i)$ evolve independently of $\mathbf{r} = (x, y)$, eventually reaching a uniform steady state for $\theta_i \in [0, 2\pi]$ for $t \gg D_i^{-1}$. On the other hand, the relaxation time-scale of distance \mathbf{r} in the harmonic trap is given by $\tau_k = 1/(2k)$. Thus, in the strongly active regime $k \gg (D_1, D_2)$, the distance vector \mathbf{r} relaxes much before the orientations \hat{n}_1, \hat{n}_2 have changed appreciably. This separation of time-scales implies that, to the first approximation, the complete stationary distribution of \mathbf{r} , in this strongly active regime, can be obtained from the conditional distribution $\mathcal{P}(\mathbf{r}|\theta_1, \theta_2)$ for fixed (θ_1, θ_2) , averaging over uniform distributions of $\{\theta_i\}$ in $[0, 2\pi]$,

$$P(\mathbf{r}) = \int_0^{2\pi} \frac{d\theta_1}{2\pi} \int_0^{2\pi} \frac{d\theta_2}{2\pi} \mathcal{P}(\mathbf{r}|\theta_1, \theta_2). \quad (10)$$

It is evident from Eq. (9), for fixed (θ_1, θ_2) , the distance vector \mathbf{r} evolves deterministically, leading to,

$$\mathcal{P}(\mathbf{r}|\theta_1, \theta_2) = \delta\left(\mathbf{r} - \frac{1}{2k} [v_1 \hat{n}_1 - v_2 \hat{n}_2]\right). \quad (11)$$

Consequently, for fixed (θ_1, θ_2) , the radial distance $r = |\mathbf{r}|$ between the two particles reaches a constant value

$$r = \frac{1}{2k} |v_1 \hat{n}_1 - v_2 \hat{n}_2|. \quad (12)$$

Clearly, r is minimum when $\theta_1 - \theta_2 = 0$, i.e., orientations of the particles are parallel and r is maximum when $\theta_1 - \theta_2 = \pi$, i.e., the particles are orientated opposite to each other. Thus, for all possible values of θ_1, θ_2 , the relative distance remains bounded in the regime given by Eq. (2) with $N = 2$. The above equation implies that particles with different self-propulsion speeds ($v_1 \neq v_2$) must be separated by a minimum distance—the strongly active nature of the dynamics gives rise to a short-range repulsive interaction, despite the strong attractive harmonic coupling.

Equations (10)-(11) allow us to compute the marginal distribution of the radial distance $r = |\mathbf{r}|$ exactly [see Appendix A for the details]

$$P(r) = \frac{2r}{\pi \sqrt{[(R^{\max})^2 - r^2][r^2 - (R^{\min})^2]}}, \quad (13)$$

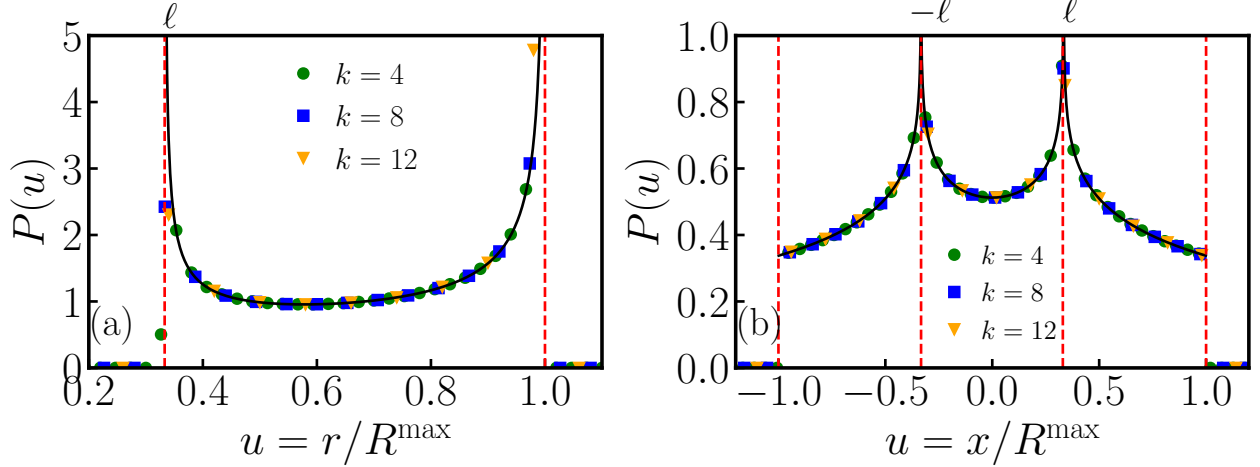


FIG. 2. Two harmonically coupled ABP: Probability distribution of (a) the radial distance and (b) the x -component of separation r obtained from numerical simulations with $v_1 = 2$, $v_2 = 4$ and $D_1 = D_2 = 0.01$. The solid black line in (a) corresponds to the scaling function Eq. (4) while the solid black line in (b) indicates the scaling function Eq. (6).

for $R^{\min} < r < R^{\max}$ which is normalized as $\int P(r)dr = 1$. Note that, Eq. (13) is equivalent to Eqs. (3) and (4) for $N = 2$. It should be emphasised that, in the strongly coupled regime, the stationary distributions are independent of the active time-scale D_i^{-1} . Figure 2(a) shows the theoretical prediction Eq. (13) along with the radial distribution obtained from numerical simulations which validates our prediction.

The rotational symmetry of the problem allows us to obtain the full two-dimensional distribution $P(x, y)$ which is illustrated in Fig. 3(a). The empty circular region around the origin ($r < R^{\min}$) indicates the dynamically inaccessible area of the phase space arising due to the repulsion.

The signature of this emergent repulsion is also visible in $P(x)$, the marginal distribution of the x -component of the distance vector r . This can also be computed analytically and is given by the scaling form [see Appendix A for the details],

$$P(x) = \frac{1}{R^{\max}} \mathcal{F}_{12} \left(\frac{x}{R^{\max}} \right), \quad (14)$$

where the scaling function $\mathcal{F}_{12}(u)$ is given in Eq. (6) with $\ell = R^{\min}/R^{\max}$. This marginal distribution has a double peaked structure with peaks at $x = \pm R^{\min}$, the emergent repulsion giving rise to a minimum at $x = 0$. The distribution shows a logarithmic divergence near the peaks. Figure 2(b) illustrates the $P(x)$ along with the same obtained from numerical simulations which shows excellent agreement.

To understand the physical origin of this repulsion, let us first note that the bounds of the distribution R^{\max} and R^{\min} correspond to the maximum and minimum of the turning points of the Langevin equation Eq. (8) for all possible values of θ_1, θ_2 . For $r > R^{\max}$, the net force is always negative, pulling the particles closer. On the other hand, for $r < R^{\min}$ the force is positive, pushing the particles apart. This push is

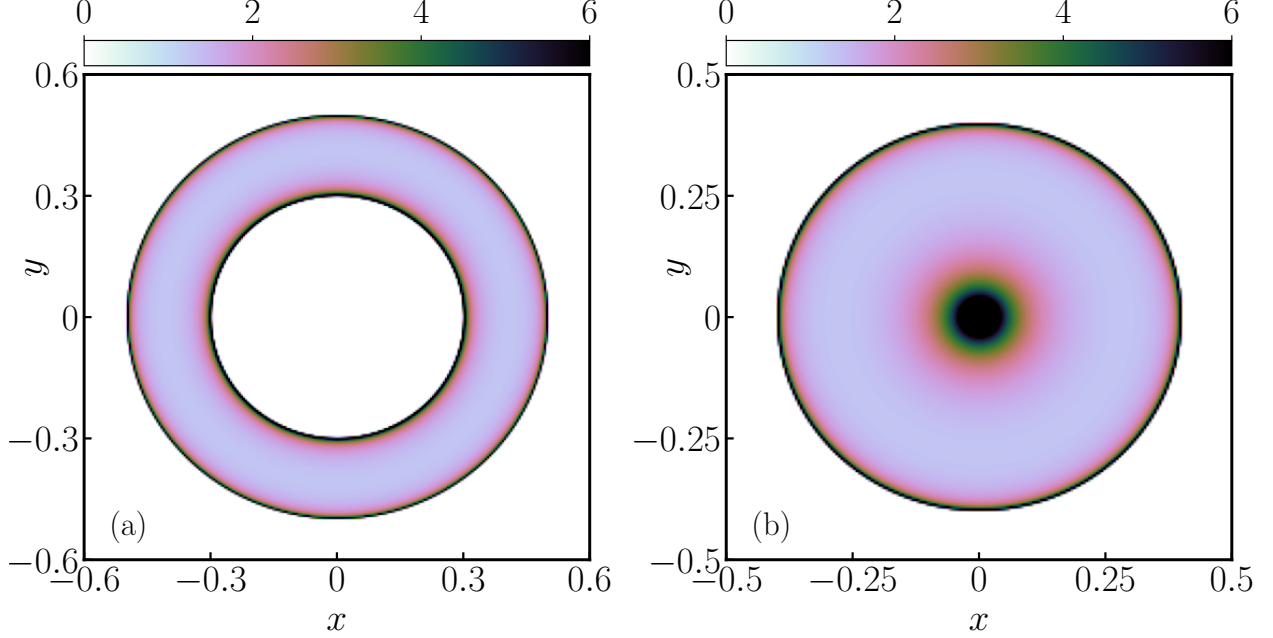


FIG. 3. Colourbar plot showing Joint distribution $P(x, y)$ for the harmonically coupled system with $N = 2$ for different values of v_1 and v_2 . The colour scale represents the value of probability $P(x, y)$. (a) $P(x, y)$ for $v_1 = 1$ and $v_2 = 4$, (b) $P(x, y)$ for $v_1 = 4$ and $v_2 = 4$. Other parameters are $k = 5$ and $D = 0.01$.

generated solely due to the difference in the self-propulsion speeds of the two particles. The presence of an upper bound for the position distribution of an active particle in the presence of an external confinement is quite common [39–42]. However, the effective repulsive interaction is a novel phenomenon, unique to the active particle dynamics, emerging due to the diversity in the self-propulsion speeds.

In fact, for the special case, $v_1 = v_2$, $R^{\min} = 0$ and Eqs. (13) - (14) reduce to

$$P(r) = \frac{2}{\pi \sqrt{v_0^2/k^2 - r^2}} \text{ for } r \leq \frac{v_0}{k}, \quad (15)$$

$$P(x) = \frac{2}{\pi^2 |x|} K \left(1 - \frac{v_0^2}{k^2 x^2} \right) \text{ for } |x| < v_0/k. \quad (16)$$

The above equations indicate that the excluded region disappears when both the particles self-propel with the same speed; see Fig. 6 in the Appendix A. In fact, $P(x)$ shows a logarithmic divergence near $x = 0$, which indicates that when the self-propulsion speed of the particles are the same, the activity leads to an increased probability of the particles being close to each other.

It is possible to extend part of the above analysis for more general, non-linear attractive interaction potentials. In this case, the Langevin equation for distance vector becomes,

$$\dot{\mathbf{r}} = -2\mathbf{f}(r) + v_1 \hat{\mathbf{n}}_1 - v_2 \hat{\mathbf{n}}_2, \quad (17)$$

where $\mathbf{f}(r) = -\nabla V(r)$. The center of mass, on the other hand, still evolves following the second equation of Eq. (8). It is expected that, for sufficiently strong attractive force $\mathbf{f}(r)$, the distance between the particles will reach a stationary state.

While it is not possible to solve Eq. (17) explicitly for arbitrary $\mathbf{f}(r)$, we can compute the bounds on r from the turning points of the Eq. (17), in the strongly active regime,. As discussed before, in the strongly active regime the active time-scale is much larger than the relaxation time-scale in the potential. Hence, one can assume that the orientations do not change appreciably in the time r relaxes in the potential. For fixed θ_i , r relaxes to the turning point of Eq. (17), given by the solution of the equation $\mathbf{f}(r^*) = (v_1 \hat{n}_1 - v_2 \hat{n}_2)/2$. This equation has a unique solution when $|f|$ is a monotonic function of r , which is true for the attractive potentials we are considering. Then, the support of the stationary distribution $P(r)$ can be obtained by considering the maximum and minimum of the turning point r^* over all possible orientations (θ_1, θ_2) , which are given by Eq. (7) [see Appendix B for the details]. Hence, for $v_1 \neq v_2$, there is always a minimum distance between the particles, indicating the emergence of the repulsion. Similar to the harmonic case, the point of nearest approach corresponds to the case $\theta_1 - \theta_2 = 0$. The corresponding stationary distribution of the distance between particles $P(r)$ as well as the marginal distribution $P(x)$ depends on the specific form of the potential.

It is important to emphasize that, although we have used the example of ABP so far, the results obtained here are expected to hold for other active particle models such as Run-and-Tumble Particles [43, 44] or direction reversing ABP [45, 46]. This is because, to show the existence of the minimum separation, we have only used the fact that in the strong coupling regime, the orientation evolves much slower than the position relaxation in the potential. Thus, the details of specific active dynamics do not play any role in this regime.

B. Multi-particle system ($N > 2$)

It is intriguing to see whether this diversity-induced repulsion survives for a system with $N > 2$ particles. First, we consider the scenario with harmonic interactions. In this case, $\mathbf{r}_{ij} \equiv \mathbf{r}_i - \mathbf{r}_j$ evolves according to the Langevin equation [see Eq. (1)],

$$\dot{\mathbf{r}}_{ij} = -Nk\mathbf{r}_{ij} + v_i\mathbf{n}_i - v_j\mathbf{n}_j. \quad (18)$$

Since the self-propulsion directions $\{\mathbf{n}_i\}$ are independent, for each pair, the above equation is equivalent to Eq. (8) with a renormalized coupling constant $\tilde{k} = Nk/2$. Then, it is straightforward to show that, in the

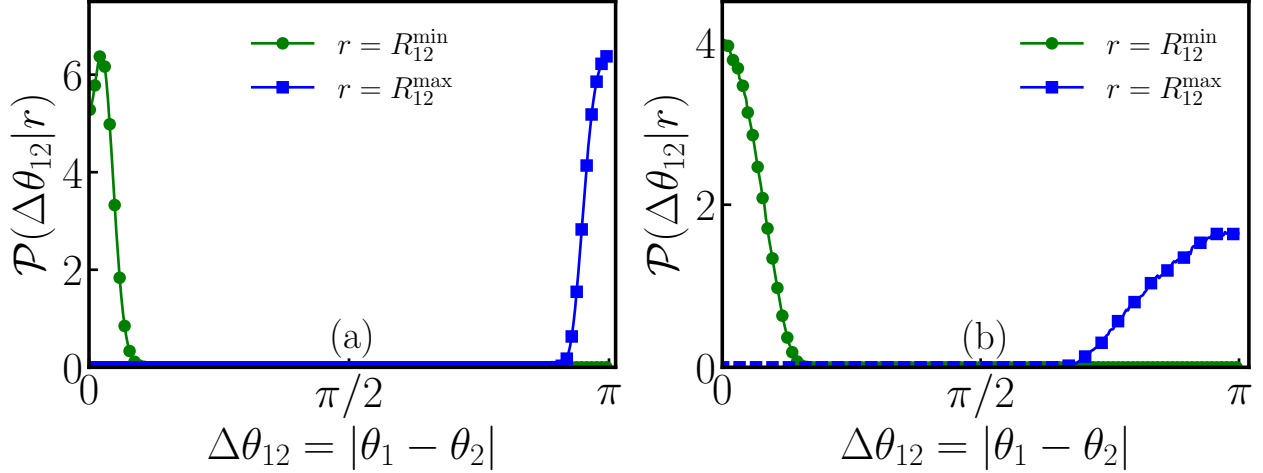


FIG. 4. Probability distribution of the relative orientation $\Delta\theta_{ij}$ for minimum and maximum separations between two particles for a system of $N = 6$ particles coupled via (a) harmonic and (b) quartic potentials. The coupling strength for harmonic potential is $k = 2$ and for quartic potential is $\kappa = 4$. The self-propulsion speed of the i -th particle is $v_i = 2i - 1$ and the rotational diffusivity of all the particles are fixed at $D_i = 0.02$.

strongly active regime $k \gg \{D_i\}$, the relative distance r_{ij} between for each pair of particles (i, j) , remains bounded in the regime defined in Eq. (2). Evidently, the stationary distributions $P(r)$ and $P(x)$ can be obtained from Eqs. (3)-(4) and Eqs. (5)-(6) respectively.

It should be emphasized that these distributions hold true for each pair of particles (i, j) . Hence, for N particles with distinct self-propulsion speeds, each particle will maintain a minimum distance from all other particles, depending on their speed difference. Seen from the centre of mass of the particles, this amounts to a finite region of the phase space being excluded.

The most interesting scenario is when $N > 2$ particles are coupled via pairwise non-linear force. In this case, the Langevin equation for r_{ij} also depends on r_{im} for all possible values of m , and it is not possible to obtain the turning points in a straightforward manner, even in the strong coupling limit. However, physically one still expects a similar behaviour for any long-range attractive coupling. We illustrate this via numerical simulations. Figure 1(a) shows a plot of the stationary distribution $P(x_{ij}, y_{ij})$ for a fixed pair $(i = 1, j = 2)$ for $N = 6$ particles interacting via the quartic potential

$$V(r) = \frac{\kappa}{4} r^4. \quad (19)$$

The emergent short-range repulsion is evident from the excluded circular region near the origin. It is also instructive to see the behaviour of the relative distance of two pairs — Figure 5 shows the joint distribution $P(r_{ij}, r_{im})$ and it is clear that the allowed region in the $r_{ij} - r_{im}$ plane is bounded by the extreme allowed values of r_{ij} and r_{im} .

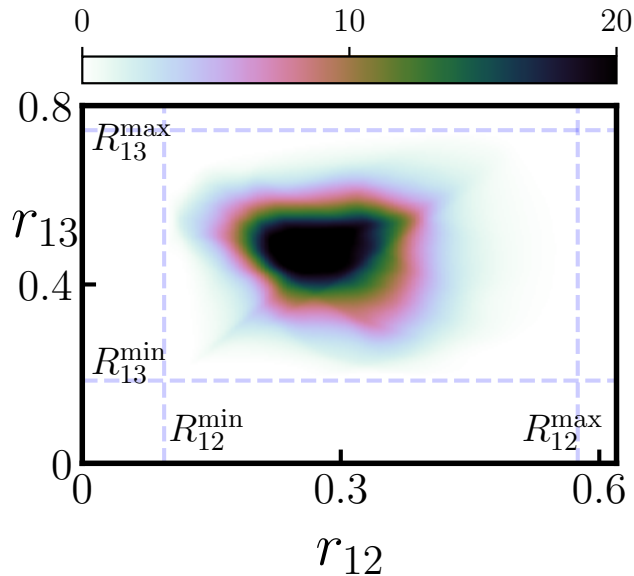


FIG. 5. Multi-particle system ($N = 6$) interacting via a pair-wise quartic potential [see Eq. (19)]: Plot of the joint distribution $P(r_{12}, r_{13})$ obtained from numerical simulations. Here we have used $v_i = 3i - 2$, $\kappa = 4$ and $D = 0.02$. We have measured the lower and upper bounds in r_{12} and r_{13} from numerical simulation. These bounds are shown using the dashed lines.

It is also interesting to investigate the relative orientation for the multi-particle case. It is previously discussed that for systems with $N = 2$ particles, the point of the nearest approach corresponds to the parallel configuration or $\theta_1 - \theta_2 = 0$ irrespective of the coupling present between the particles. Figure 4 shows the distribution of the relative orientation $\Delta\theta_{ij} = \theta_i - \theta_j$ between the particles (i, j). Fig. 4(a) shows the orientation distribution for the harmonically coupled system which shows that the point of closest and farthest approach corresponds to parallel and anti-parallel configuration respectively. Similar result is shown in Fig. 4(b) for the system with attractive interaction potential Eq. (19).

III. CONCLUSION

We show that a novel short-repulsion emerges for attractively coupled active particles in the presence of diversity in self-propulsion speeds. Numerical evidence provided in a recent work [47] suggests that diversity in propulsion speed opposes cluster formation. Our study provides the first theoretical attempt to explore the microscopic origin of such a phenomenon. Our findings are also consistent with the recent observation that presence of attractive interaction hinders the formation of clusters in active systems [48, 49]. The emergence of short-range repulsion among coupled active particles gives rise to novel possibilities for collective phenomena like structure formation which needs to be explored further.

ACKNOWLEDGMENTS

R.S. acknowledges CSIR Grant No. 09/0575(11358)/2021-EMR-I. U.B. acknowledges support from the Anusandhan National Research Foundation (ANRF), India, under a MATRICS grant [No. MTR/2023/000392].

Appendix A: Computation of stationary separation distribution for harmonic coupling

In this section, we provide the detailed derivation leading to the stationary distribution $P(r)$ and $P(x)$ quoted in Eqs. (3)- (6). We start with the radial distribution $P(r)$ for $N = 2$ particle case. In the strong-coupling regime, we have from Eq. (12), for fixed (θ_1, θ_2) ,

$$r = \frac{1}{2k} \sqrt{v_1^2 + v_2^2 - 2v_1v_2 \cos(\theta_1 - \theta_2)}. \quad (\text{A1})$$

Consequently, we have,

$$\mathcal{P}(r|\theta_1, \theta_2) = \delta \left(r - \frac{1}{2k} \sqrt{v_1^2 + v_2^2 - 2v_1v_2 \cos(\theta_1 - \theta_2)} \right). \quad (\text{A2})$$

To obtain $P(r)$ we need to average over all possible values of θ_1, θ_2 drawn from independent uniform distributions in $[0, 2\pi]$ [see Eq. (10)]. To this end, we first note that for two independent and identically distributed uniform random variables θ_1 and θ_2 , the variable $s = \cos(\theta_1 - \theta_2)$ has the probability distribution,

$$\rho(s) = \frac{1}{\pi\sqrt{1-s^2}}, \quad (\text{A3})$$

which is supported over the region $-1 \leq s \leq 1$. Using the above equation in Eq. (10), we have,

$$P(r) = \int_{-1}^1 \frac{ds}{\pi\sqrt{1-s^2}} \delta \left(r - \frac{1}{2k} \sqrt{v_1^2 + v_2^2 - 2v_1v_2s} \right). \quad (\text{A4})$$

Evaluating the s -integral, we finally get,

$$P(r) = \frac{4k^2 r}{\pi v_1 v_2 \sqrt{1-s^{*2}}}. \quad (\text{A5})$$

where, $s^* = (4k^2 r^2 - v_1^2 - v_2^2)/(2v_1v_2)$ denotes the point in the region $[-1, 1]$ where the argument of the delta-function vanishes. The explicit form of $P(r)$ is quoted in Eq. (13). For $v_1 = v_2 = v_0$, $s^* = 2k^2 r^2/v_0^2$ and the radial distribution reduces to Eq. (15).

Next, we compute the marginal distribution of the x -component of the separation vector \mathbf{r} . In the strong-coupling limit, for fixed (θ_1, θ_2) , we have from Eq (9),

$$x = a_1 \cos \theta_1 - a_2 \cos \theta_2, \text{ where, } a_i = \frac{v_i}{2k}. \quad (\text{A6})$$

The conditional distribution $\mathcal{P}(x|\theta_1, \theta_2)$ is then given by,

$$\mathcal{P}(x|\theta_1, \theta_2) = \delta(x - a_1 \cos \theta_1 + a_2 \cos \theta_2). \quad (\text{A7})$$

The marginal probability distribution of x -component, thus, is given by,

$$P(x) = \int_{-\infty}^{\infty} dz_1 \int_{-\infty}^{\infty} dz_2 \delta(x - a_1 z_1 + a_2 z_2) \rho(z_1) \rho(z_2), \quad (\text{A8})$$

where $z_i = \cos \theta_i$. It is straightforward to show that the distribution of z_i is nothing but $\rho(z_i)$, given in Eq. (A3). Using Eq. (A3) in Eq. (A8) and integrating over z_2 , we arrive at,

$$P(x) = \frac{1}{a_1 \pi^2} \int_{-1}^1 dz_1 \frac{\Theta(z_1 - b_1)}{\sqrt{1 - z_1^2}} \frac{\Theta(b_2 - z_1)}{\sqrt{(z_1 - b_1)(b_2 - z_1)}}, \quad (\text{A9})$$

where $\Theta(z)$ is the Heaviside theta function. We have also defined $b_1 = (x - a_2)/a_1$ and $b_2 = (x + a_2)/a_1$ for notational simplicity. The above integral can be evaluated exactly and leads to,

$$P(x) = \begin{cases} \frac{2i}{\pi^2 \sqrt{(R^{\min})^2 - x^2}} \left[K \left(\frac{(R^{\max})^2 - x^2}{(R^{\min})^2 - x^2} \right) - \sqrt{\frac{(R^{\min})^2 - x^2}{(R^{\max})^2 - x^2}} K \left(\frac{(R^{\min})^2 - x^2}{(R^{\max})^2 - x^2} \right) \right] & \text{for } |x| < R^{\max}, \\ \frac{2}{\pi^2 \sqrt{x^2 - (R^{\min})^2}} K \left[\frac{(R^{\max})^2 - x^2}{(R^{\min})^2 - x^2} \right] & \text{for } R^{\min} < |x| < R^{\max}, \end{cases} \quad (\text{A10})$$

where $K(u)$ denotes the complete Elliptic integral of the first kind [38]. This distribution shows a logarithmic divergence near the peaks at $x = \pm R^{\min}$,

$$P(x) \simeq \frac{-\log |x - R^{\min}| + \log [(R^{\max})^2 - (R^{\min})^2]}{\sqrt{(R^{\max})^2 - (R^{\min})^2}}. \quad (\text{A11})$$

For the special case $\nu_1 = \nu_2 = \nu_0$, we have $R^{\min} = 0, R^{\max} = \nu_0/k$. The marginal distribution, in this case, is given by,

$$P(x) = \begin{cases} \frac{2k}{\pi^2 \nu_0} \int_{2kx/\nu_0-1}^1 \frac{dz}{\sqrt{1-z^2} \sqrt{(z-c_1)(c_2-z)}} & \text{for } 0 < x \leq \frac{\nu_0}{k}, \\ \frac{2k}{\pi^2 \nu_0} \int_{-1}^{2kx/\nu_0+1} \frac{dz}{\sqrt{1-z^2} \sqrt{(z-c_1)(c_2-z)}} & \text{for } -\frac{\nu_0}{k} \leq x < 0, \end{cases} \quad (\text{A12})$$

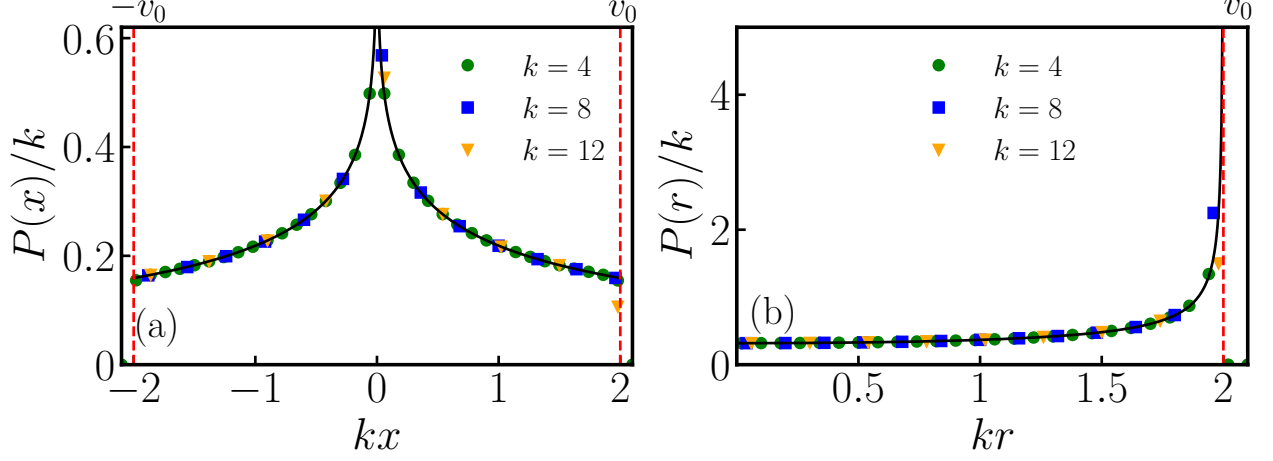


FIG. 6. Scaled plot of (a) $P(x)$ and (b) $P(r)$ for the harmonically coupled two-particle case with $v_1 = v_2$. The black solid lines in (a) and (b) correspond to Eq. (16) and Eq. (15), respectively. Here we have taken $v_1 = v_2 = 2$ and $D_1 = D_2 = 0.01$.

where, $c_1 = (2kx - v_0)/v_0$ and $c_2 = (2kx + v_0)/v_0$. After performing the integral we arrive at Eq. (16). The distribution in Eq. (16) shows a logarithmic divergence near $x = 0$,

$$P(x) \simeq \frac{2k}{\pi^2 v_0} \left(-\log x + \log \frac{4v_0}{k} \right). \quad (\text{A13})$$

The radial and x -marginal distributions for the $v_1 = v_2$ case are illustrated in Fig. 6.

Appendix B: Estimation of the minimum separation for anharmonic coupling

The equation of motion of the radial distance between two ABPs coupled to each other by a long-range attractive force $\mathbf{f}(r)$ is given by

$$\dot{\mathbf{r}}_{12} = -2\mathbf{f}(r_{12}) + v_1 \hat{\mathbf{n}}_1 - v_2 \hat{\mathbf{n}}_2, \quad (\text{B1})$$

where $\hat{\mathbf{n}}_i = (\cos \theta_i, \sin \theta_i)$ indicates the internal orientation of the ABPs. In the strong coupling limit, the distance vector \mathbf{r} relaxes in the attractive potential much before the orientations $\hat{\mathbf{n}}_1, \hat{\mathbf{n}}_2$ have changed appreciably. For any fixed (θ_1, θ_2) , the radial distance eventually approaches the turning point r^* , which satisfies,

$$f(r^*) = \frac{1}{2} \sqrt{[v_1^2 + v_2^2 - 2v_1 v_2 \cos(\theta_1 - \theta_2)]}, \quad (\text{B2})$$

where $f(r) = |\mathbf{f}(r)|$. Clearly, for monotonically increasing functions $f(r)$, which we are considering, Eq. (B2) implies Eq. (7) quoted in the main text. Especially, for the anharmonic potential (19), we have,

$$R^{\min} = \left(\frac{|v_1 - v_2|}{2\kappa} \right)^{\frac{1}{3}}, \quad \text{and} \quad R^{\max} = \left(\frac{v_1 + v_2}{2\kappa} \right)^{\frac{1}{3}}. \quad (\text{B3})$$

-
- [1] P. Romanczuk, M. Bär, W. Ebeling, B. Lindner, and L. Schimansky-Geier, *The European Physical Journal Special Topics* **202**, 1 (2012).
- [2] Étienne Fodor and M. C. Marchetti, *Physica A: Statistical Mechanics and its Applications* **504**, 106 (2018), lecture Notes of the 14th International Summer School on Fundamental Problems in Statistical Physics.
- [3] S. Ramaswamy, *Annual Review of Condensed Matter Physics* **1**, 323 (2010).
- [4] M. C. Marchetti, J. F. Joanny, S. Ramaswamy, T. B. Liverpool, J. Prost, M. Rao, and R. A. Simha, *Rev. Mod. Phys.* **85**, 1143 (2013).
- [5] C. Bechinger, R. Di Leonardo, H. Löwen, C. Reichhardt, G. Volpe, and G. Volpe, *Rev. Mod. Phys.* **88**, 045006 (2016).
- [6] J. O’Byrne, Y. Kafri, J. Tailleur, and F. van Wijland, *Nature Reviews Physics* **4**, 167 (2022).
- [7] J. Elgeti, R. G. Winkler, and G. Gompper, *Reports on Progress in Physics* **78**, 056601 (2015).
- [8] H. C. Berg, *E. coli in Motion* (Springer, 2004).
- [9] A. Cavagna and I. Giardina, *Annual Review of Condensed Matter Physics* **5**, 183 (2014).
- [10] J. Toner and Y. Tu, *Phys. Rev. Lett.* **75**, 4326 (1995).
- [11] J. Toner, Y. Tu, and S. Ramaswamy, *Annals of Physics* **318**, 170 (2005), special Issue.
- [12] A. Filella, F. m. c. Nadal, C. Sire, E. Kanso, and C. Eloy, *Phys. Rev. Lett.* **120**, 198101 (2018).
- [13] M. Jiang, A. Zhou, R. Chen, Y. Yang, H. Dong, and W. Wang, *Phys. Rev. E* **107**, 024411 (2023).
- [14] X. Zheng, B. ten Hagen, A. Kaiser, M. Wu, H. Cui, Z. Silber-Li, and H. Löwen, *Phys. Rev. E* **88**, 032304 (2013).
- [15] M. N. van der Linden, L. C. Alexander, D. G. A. L. Aarts, and O. Dauchot, *Phys. Rev. Lett.* **123**, 098001 (2019).
- [16] M. E. Cates and J. Tailleur, *Annual Review of Condensed Matter Physics* **6**, 219 (2015).
- [17] H. Löwen, *The Journal of Chemical Physics* **152**, 040901 (2020).
- [18] P. Digregorio, D. Levis, A. Suma, L. F. Cugliandolo, G. Gonnella, and I. Pagonabarraga, *Physical review letters* **121**, 098003 (2018).
- [19] L. Caprini, U. Marini Bettolo Marconi, and A. Puglisi, *Phys. Rev. Lett.* **124**, 078001 (2020).
- [20] T. Vicsek and A. Zafeiris, *Physics Reports* **517**, 71 (2012), collective motion.
- [21] T. Vicsek, A. Czirók, E. Ben-Jacob, I. Cohen, and O. Shochet, *Phys. Rev. Lett.* **75**, 1226 (1995).
- [22] J. Toner and Y. Tu, *Phys. Rev. E* **58**, 4828 (1998).
- [23] J. Palacci, S. Sacanna, A. P. Steinberg, D. J. Pine, and P. M. Chaikin, *Science* **339**, 936 (2013).
- [24] N. Kumar, R. K. Gupta, H. Soni, S. Ramaswamy, and A. K. Sood, *Phys. Rev. E* **99**, 032605 (2019).
- [25] P. B. Sapat and S. Mishra, *Phys. Rev. E* **104**, 024130 (2021).
- [26] M. P. Umberto Marini Bettolo Marconi and C. Maggi, *Molecular Physics* **114**, 2400 (2016), <https://doi.org/10.1080/00268976.2016.1155777>.
- [27] A. B. Slowman, M. R. Evans, and R. A. Blythe, *Phys. Rev. Lett.* **116**, 218101 (2016).
- [28] A. Slowman, M. Evans, and R. Blythe, *Journal of Physics A: Mathematical and Theoretical* **50**, 375601 (2017).

- [29] E. Mallmin, R. A. Blythe, and M. R. Evans, *Journal of Statistical Mechanics: Theory and Experiment* **2019**, 013204 (2019).
- [30] A. Das, A. Dhar, and A. Kundu, *Journal of Physics A: Mathematical and Theoretical* **53**, 345003 (2020).
- [31] P. Le Doussal, S. N. Majumdar, and G. Schehr, *Physical Review E* **104**, 044103 (2021).
- [32] M. J. Metson, M. R. Evans, and R. A. Blythe, *Europhysics Letters* **141**, 41001 (2023).
- [33] M. J. Metson, M. R. Evans, and R. A. Blythe, *Phys. Rev. E* **107**, 044134 (2023).
- [34] M. J. Metson, M. R. Evans, and R. A. Blythe, *Journal of Statistical Mechanics: Theory and Experiment* **2020**, 103207 (2020).
- [35] U. Basu, S. N. Majumdar, A. Rosso, and G. Schehr, *Phys. Rev. E* **98**, 062121 (2018).
- [36] K. Malakar, A. Das, A. Kundu, K. V. Kumar, and A. Dhar, *Phys. Rev. E* **101**, 022610 (2020).
- [37] U. Basu, S. N. Majumdar, A. Rosso, and G. Schehr, *Phys. Rev. E* **100**, 062116 (2019).
- [38] DLMF, *NIST Digital Library of Mathematical Functions*, <https://dlmf.nist.gov/>, Release 1.2.3 of 2024-12-15, f. W. J. Olver, A. B. Olde Daalhuis, D. W. Lozier, B. I. Schneider, R. F. Boisvert, C. W. Clark, B. R. Miller, B. V. Saunders, H. S. Cohl, and M. A. McClain, eds.
- [39] N. Narinder, J. R. Gomez-Solano, and C. Bechinger, *New Journal of Physics* **21**, 093058 (2019).
- [40] A. Choudhary, K. Chaithanya, S. Michelin, and S. Pushpavanam, *The European Physical Journal E* **44**, 1 (2021).
- [41] S. C. Takatori, R. De Dier, J. Vermant, and J. F. Brady, *Nature communications* **7**, 10694 (2016).
- [42] M. Mijalkov, A. McDaniel, J. Wehr, and G. Volpe, *Phys. Rev. X* **6**, 011008 (2016).
- [43] K. Malakar, V. Jemseena, A. Kundu, K. V. Kumar, S. Sabhapandit, S. N. Majumdar, S. Redner, and A. Dhar, *Journal of Statistical Mechanics: Theory and Experiment* **2018**, 043215 (2018).
- [44] J. Tailleur and M. E. Cates, *Phys. Rev. Lett.* **100**, 218103 (2008).
- [45] I. Santra, U. Basu, and S. Sabhapandit, *Phys. Rev. E* **104**, L012601 (2021).
- [46] I. Santra, U. Basu, and S. Sabhapandit, *Soft Matter* **17**, 10108 (2021).
- [47] P. de Castro, F. M. Rocha, S. Diles, R. Soto, and P. Sollich, *Soft Matter* **17**, 9926 (2021).
- [48] I. Mukherjee, A. Raghu, and P. K. Mohanty, *SciPost Phys.* **14**, 165 (2023).
- [49] C. G. Ray, I. Mukherjee, and P. K. Mohanty, *Journal of Statistical Mechanics: Theory and Experiment* **2024**, 093207 (2024).